3ω method for specific heat and thermal conductivity measurements

L. Lu, W. Yi, and D. L. Zhang

Citation: Review of Scientific Instruments **72**, 2996 (2001);
View online: https://doi.org/10.1063/1.1378340
View Table of Contents: http://aip.scitation.org/toc/rsi/72/7
Published by the American Institute of Physics

3ω method for specific heat and thermal conductivity measurements

L. Lu,[a] W. Yi, and D. L. Zhang
Laboratory of Extreme Conditions Physics, Institute of Physics and Center for Condensed Matter Physics, Chinese Academy of Sciences, Beijing 100080, People's Republic of China

(Received 23 February 2000; accepted for publication 16 April 2001)

We present a 3ω method for simultaneously measuring the specific heat and thermal conductivity of a rod- or filament-like specimen using a way similar to a four-probe resistance measurement. The specimen in this method needs to be electrically conductive and with a temperature-dependent resistance, for acting both as a heater to create a temperature fluctuation and as a sensor to measure its thermal response. With this method, we have successfully measured the specific heat and thermal conductivity of platinum wire specimens at cryogenic temperatures, and measured those thermal quantities of tiny carbon nanotube bundles some of which are only $\sim 10^{-9}$ g in mass. © *2001 American Institute of Physics.* [DOI: 10.1063/1.1378340]

I. INTRODUCTION

Many experimental methods have been developed over the past centuries to measure the fundamental thermal properties of materials. One important class among them, the so-called 3ω method, uses a narrow-band detection technique and therefore gives a relatively better signal-to-noise ratio. In this method, either the specimen itself serves as a heater and at the same time a temperature sensor, if it is electrically conductive and with a temperature-dependent electric resistance, or for electrically nonconductive specimen, a metal strip is artificially deposited on its surface to serve both as the heater and the sensor. Feeding an ac electric current of the form $I_0 \sin \omega t$ into the specimen or the metal strip creates a temperature fluctuation on it at the frequency 2ω, and accordingly a resistance fluctuation at 2ω. This further leads to a voltage fluctuation at 3ω across the specimen. Corbino[1] is probably the first to notice that the temperature fluctuation of an ac heated wire gives useful information about the thermal properties of the constituent material. Systematic investigations of the 3ω method were carried out mainly during the 1960's[2–4] and in the last ten years,[5–10] which made the method practical. However, in the previous studies the heat-conduction equation was solved under the approximations either only for the high frequency limit,[2,3,10] or only for the low frequency limit.[5,7,8] With those approximations one lost either the information on the thermal conductivity or the information on the specific heat of the specimen.

In this article, we present an explicit solution for the one-dimensional(1D) heat-conduction equation. With this solution and by using a modern digital lock-in amplifier, we are able to obtain both the specific heat and the thermal conductivity of a rod- or filament-like specimen simultaneously. We have tested this method on platinum wire specimens. Correct values of specific heat, thermal conductivity, and Wiedemenn–Franz ratio were obtained. With this method, we have also obtained the thermal properties of carbon nanotube bundles some of which are only 10^{-9} g in mass.

[a]Electronic mail: lilu@aphy.iphy.ac.cn

In Sec. II, we will present an explicit solution for the 1D heat-conduction equation. In Sec. III, we will discuss the high and low frequency limits of the solution, then compare them with the ones previously obtained by others at these limits. An error analysis will be given in Sec. IV, for the case of just keeping the first term of the solution. In Sec. V, we will discuss the effects of radial heat loss. And, in Sec. VI, we will show our experimental test of the method on platinum and carbon nanotube materials. We will also share with the readers the tips of using this 3ω method.

II. THE 1D HEAT CONDUCTION EQUATION AND ITS SOLUTION

We consider a uniform rod- or filament-like specimen in a four-probe configuration as for electrical resistance measurement (Fig. 1). The two outside probes are used for feeding an electric current, and the two inside ones for measuring the voltage across the specimen. Differing from being a pure electrical resistance measurement, however, here it requires that (i) the specimen in between the two voltage probes be suspended to allow the temperature fluctuation, (ii) all the probes have to be highly thermal conductive, to heat sink the specimen at these points to the sapphire substrate, and (iii) the specimen has to be maintained in a high vacuum and the whole setup be heat shielded to the substrate temperature to minimize the radial heat loss through gas convection and radiation. In such a configuration and with an ac electrical current of the form $I_0 \sin \omega t$ passing through the specimen, the heat generation and diffusion along the specimen can be described by the following partial differential equation and the initial and boundary conditions:

$$\rho C_p \frac{\partial}{\partial t} T(x,t) - \kappa \frac{\partial^2}{\partial x^2} T(x,t) = \frac{I_0^2 \sin^2 \omega t}{LS} [R + R'(T(x,t) - T_0)], \quad (1)$$

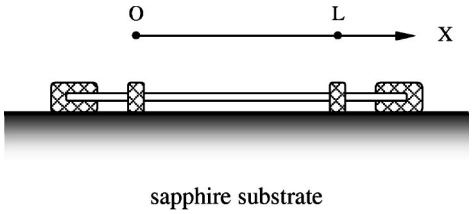

FIG. 1. Illustration of the four-probe configuration for measuring the specific heat and thermal conductivity of a rod- or filament-like specimen is shown. The specimen is heat sunk to the sapphire substrate through the four electric contacts, but the part in between the two voltage contacts needs to be suspended, to allow the temperature variation. A high vacuum is needed and a thermal shielding is preferred to eliminate the radial heat current from the specimen to the environment.

$$\begin{cases} T(0,t)=T_0 \\ T(L,t)=T_0 \\ T(x,-\infty)=T_0, \end{cases} \tag{2}$$

where C_p, κ, R, and ρ are the specific heat, thermal conductivity, electric resistance and mass density of the specimen at the substrate temperature T_0, respectively. $R'=(dR/dT)_{T_0}$. L is the length of the specimen between voltage contacts, and S the cross section of the specimen. We have assumed that the electric current was turned on at $t=-\infty$.

Let $\Delta(x,t)$ denote the temperature variation from T_0, i.e., $\Delta(x,t)=T(x,t)-T_0$, Eqs. (1) and (2) then become

$$\frac{\partial}{\partial t}\Delta(x,t)-\alpha\frac{\partial^2}{\partial x^2}\Delta(x,t)-c\sin^2\omega t \quad \Delta(x,t)=b\sin^2\omega t, \tag{3}$$

$$\begin{cases} \Delta(0,t)=0 \\ \Delta(L,t)=0 \\ \Delta(x,-\infty)=0, \end{cases} \tag{4}$$

where $\alpha=\kappa/\rho C_p$ is the thermal diffusivity, and $b=I_0^2R/\rho C_pLS$, $c=I_0^2R'/\rho C_pLS$.

Using the impulse theorem, $\Delta(x,t)$ can be represented as the integral of the responses of the specimen to the instant ''force'' $b\sin^2\omega t$ at each time interval:

$$\Delta(x,t)=\int_{-\infty}^{t} z(x,t;\tau)d\tau, \tag{5}$$

where $z(x,t;\tau)$ satisfies

$$\frac{\partial z}{\partial t}-\alpha\frac{\partial^2 z}{\partial x^2}-c\sin^2\omega t\, z=0, \tag{6}$$

$$\begin{cases} z(0,t)=0 \\ z(L,t)=0 \\ z(x,\tau+0)=b\sin^2\omega\tau. \end{cases} \tag{7}$$

$z(x,t;\tau)$ can be expanded in the Fourier series:

$$z(x,t;\tau)=\sum_{n=1}^{\infty} U_n(t;\tau)\sin\frac{n\pi x}{L}. \tag{8}$$

Substituting Eq. (8) into Eq. (6), we have

$$\sum_{n=1}^{\infty}\left[\frac{dU_n}{dt}+\left(\frac{n^2}{\gamma}-c\sin^2\omega t\right)U_n\right]\sin\frac{n\pi x}{L}=0, \tag{9}$$

where $\gamma\equiv L^2/\pi^2\alpha$ is the characteristic thermal time constant of the specimen for the axial thermal process.

The term $c\sin^2\omega t$ can be neglected if $n^2/\gamma\gg c$, or equivalently

$$\frac{I_0^2R'L}{n^2\pi^2\kappa S}\ll 1. \tag{10}$$

Condition (10) means that the heating power inhomogeneity caused by resistance fluctuation along the specimen should be much less than the total heat power. This condition is usually held. For example, in a typical measurement one could have $I_0=10\,\mathrm{mA}$, $R'=0.1\,\Omega/\mathrm{K}$, $L=1\,\mathrm{mm}$, $S=10^{-2}\,\mathrm{mm}^2$, and $\kappa=100\,\mathrm{W/m\,K}$, the left-hand side of Eq. (10) is then about 10^{-3} even for the $n=1$ case.

After dropped off the $c\sin^2\omega t$ term, the solution of the ordinary differential Eq. (9) is

$$U_n(t;\tau)=C_n(\tau)e^{-(n^2/\gamma)(t-\tau)}, \tag{11}$$

where $C_n(\tau)$ can be determined using the initial condition in Eq. (7), together with the relation $\Sigma_{n=1}^{\infty}\{2[1-(-1)^n]/n\pi\}\sin n\pi x/L=1$ for $0<x<L$:

$$C_n(\tau)=\frac{2b[1-(-1)^n]}{n\pi}\sin^2\omega\tau. \tag{12}$$

Using Eqs. (11) and (12), Eq. (8) becomes

$$z(x,t;\tau)=\sum_{n=1}^{\infty}\sin\frac{n\pi x}{L}\,\frac{2b[1-(-1)^n]}{n\pi}\,\sin^2\omega\tau\;e^{-(n^2/\gamma)(t-\tau)}. \tag{13}$$

Substituting Eq. (13) into Eq. (5) and remembering that $\Delta(x,t)=T(x,t)-T_0$, we obtain the temperature distribution along the specimen:

$$T(x,t)-T_0=\Delta_0\sum_{n=1}^{\infty}\frac{[1-(-1)^n]}{2n^3}\times\sin\frac{n\pi x}{L}\left[1-\frac{\sin(2\omega t+\phi_n)}{\sqrt{1+\cot^2\phi_n}}\right], \tag{14}$$

where $\cot\phi_n=2\omega\gamma/n^2$, and $\Delta_0=2\gamma b/\pi=2I_0^2R/(\pi\kappa S/L)$ is the maximum dc temperature accumulation at the center of the specimen. Δ_0 is only κ dependent. The information of C_p is included in the fluctuation amplitude of the temperature around the dc accumulation.

Figure 2 illustrates how the amplitude of such a temperature fluctuation depends on the frequency of the electric current. The amplitude reaches the maximum as $\omega\gamma\to 0$, i.e., when the thermal wavelength $\lambda\gg L$ (where λ is defined as $\lambda=\sqrt{\alpha/2\omega}$). But it shrinks to zero along the line of the averaged temperature accumulation when $\omega\gamma\gg 1$ ($\lambda\ll L$).

The temperature fluctuation will result in a resistance fluctuation, which can be calculated as

$$\delta R=\frac{R'}{L}\int_0^L[T(x,t)-T_0]dx. \tag{15}$$

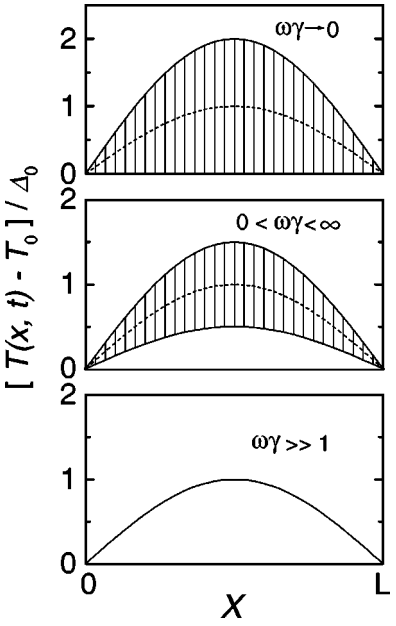

FIG. 2. Temperature fluctuation along the specimen under a driving ac current $I_0 \sin \omega t$ is shown. The fluctuation amplitude is marked as shadowed area. It reaches the maximum at the limit $\omega\gamma \to 0$, and shrinks to a line as $\omega\gamma \to \infty$. The line in the middle of the fluctuation range denotes the dc temperature accumulation along the specimen, which reaches the maximum value of Δ_0 (defined in the text) at the center of the specimen.

Using Eq. (14) and the relation $\int_0^L (\sin n\pi x/L)\,dx = [1-(-1)^n]L/n\pi$, the resistance fluctuation can be expressed as

$$\delta R = R'\Delta_0 \sum_{n=1}^{\infty} \frac{[1-(-1)^n]^2}{2\pi n^4}\left[1 - \frac{\sin(2\omega t+\phi_n)}{\sqrt{1+\cot^2\phi_n}}\right]. \quad (16)$$

As a product of the total resistance $R+\delta R$ and the current $I_0 \sin \omega t$, the voltage across the specimen contains a 3ω component $V_{3\omega}(t)$. Obviously, the $n=2$ term in $V_{3\omega}(t)$ automatically vanishes. If only taking the $n=1$ term, which introduces a relative error of the order $\sim 3^{-4}$ at low frequencies, we have

$$V_{3\omega}(t) \approx -\frac{2I_0^3 LRR'}{\pi^4 \kappa S\sqrt{1+(2\omega\gamma)^2}} \sin(3\omega t - \phi), \quad (17)$$

where we have redefined the phase constant $\phi = \frac{\pi}{2} - \phi_1$ so that

$$\tan\phi \approx 2\omega\gamma. \quad (18)$$

If using the root-mean-square (rms) values of voltage and current as what the lock-in amplifier gives, Eq. (17) becomes (hereafter we always let $V_{3\omega}$ denotes the rms value of $V_{3\omega}(t)$, and I denotes the rms value of $I_0 \sin \omega t$):

$$V_{3\omega} \approx \frac{4I^3 LRR'}{\pi^4 \kappa S\sqrt{1+(2\omega\gamma)^2}}. \quad (19)$$

By fitting the experimental data to this formula, we can get the thermal conductivity κ and thermal time constant γ of the specimen. The specific heat can then be calculated as

$$C_p = \pi^2 \gamma\kappa/\rho L^2. \quad (20)$$

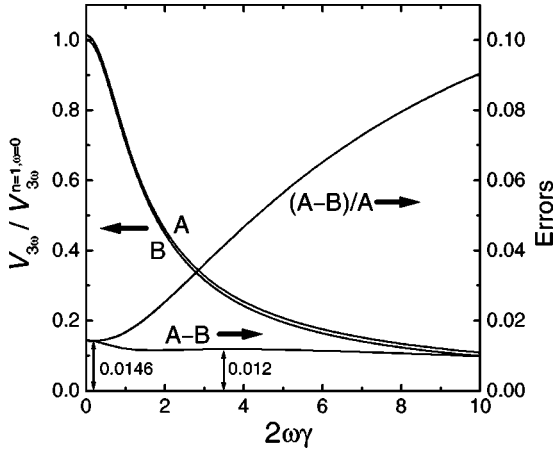

FIG. 3. The errors of $V_{3\omega}$ caused by truncating the $n>1$ terms in Eq. (16) are shown. Curve A represents the exact solution of the 3ω voltage amplitude. Curve B is the 3ω voltage of the $n=1$ term alone. The difference between them is nearly a constant at low frequencies, plotted as curve A–B. The relative error of $V_{3\omega}$ increases with ω, illustrated as curve (A–B)/A.

The following alternative form makes it more clear how the 3ω voltage depends on the dimensions of the specimen:

$$V_{3\omega} \approx \frac{4I^3\rho_e\rho_e'}{\pi^4\kappa\sqrt{1+(2\omega\gamma)^2}}\left(\frac{L}{S}\right)^3, \quad (21)$$

where ρ_e is the electrical resistivity of the specimen, $\rho_e' \equiv (d\rho_e/dT)$.

III. THE HIGH AND LOW FREQUENCY LIMITS

Sometimes the measurement has to be performed at the low frequency limit $\omega\gamma \to 0$ ($\lambda \gg L$), e.g., when the specimen is extremely thin and long. In this case, $V_{3\omega}$ is nearly frequency independent. To an accuracy of roughly 3^{-4}, it takes the form

$$V_{3\omega} \approx \frac{4I^3 RR' L}{\pi^4 \kappa S} = \frac{1}{\pi^3} IR'\Delta_0 \quad (\omega\gamma \to 0). \quad (22)$$

If the measurement is performed at the low frequency limit, one can only get the thermal conductivity of the specimen, but loses the information on specific heat, as in Cahill's treatment for a two-dimensional heat diffusion problem.[8]

At the high frequency limit $\omega\gamma \to \infty$ ($\lambda \ll L$), on the other hand, Eqs. (17)–(21) become quite inaccurate due to truncating the $n>1$ terms in Eq. (16). In this limit, all the ϕ_n approach to zero, and the amplitude of the summation over the time-dependent terms in Eq. (16) eventually becomes $\Sigma_{n=1,\text{odd}}^{\infty} n^{-2} = \pi^2/8$. Therefore, $V_{3\omega}$ should be

$$V_{3\omega} = \frac{I^3 RR'}{4\omega\rho C_p LS} \quad (\omega\gamma \to \infty), \quad (23)$$

which is exactly the same as Holland's result.[2] Simply truncating the $n>1$ terms at the $\omega\gamma \to \infty$ limit will result in a coefficient of $2/\pi^2$, instead of 1/4, for $V_{3\omega}$ in Eq. (23).

At the high frequency limit, one can only get the specific heat of the specimen, but loses the information on its thermal conductivity.

IV. ERROR ANALYSIS

The error of $V_{3\omega}$ caused by truncating the $n>1$ terms in Eq. (16) is illustrated in Fig. 3. Curve A is the normalized fluctuation amplitude of Eq. (16) containing terms up to $n=9$, taken from a numerically generated time sequence. It almost represents the exact solution. Curve B is the fluctuation amplitude of the first term alone. It appears that the difference between A and B (shown as curve A–B in Fig. 3) is nearly a constant in the frequency range $0<2\omega\gamma<10$. It approaches to $\Sigma_{n=3,\text{odd}}^{\infty} n^{-4}\approx 0.014$ as $\omega\rightarrow 0$. However, because $V_{3\omega}$ decreases with frequency, the relative error of $V_{3\omega}$ increases with ω (illustrated as curve (A–B)/A in Fig. 3).

The relative error of $\tan\phi$ in Eq. (18) should also increase with frequency. Indeed, the experimental data of $\tan\phi$ curve away from linearity at high frequencies. By fitting the data to Eq. (18), the high frequency inaccurate side of Eq. (18) provides more weight on the slope, so that one will get a noticeably smaller γ than the true value.

The case of using Eq. (19) is fortunately just the opposite. The amplitude of $V_{3\omega}$ is relatively large at the low frequency side where Eq. (19) is very accurate. If we fit curve A to Eq. (19) in the frequency range $0<2\omega\gamma<4$, the obtained κ is only 3.5% higher, and γ is 2% lower than the true values. C_p is then only 1.4% higher than the true value.

Because the error in Eq. (19) is nearly frequency independent at low frequencies (curve A–B in Fig. 3), it can be further and easily reduced by shifting the fitting curve upwards by a small amount, i.e., fitting the data to the following form:[11]

$$V_{3\omega}\approx \frac{4I^3LRR'}{1.01\pi^4\kappa S}\left[\frac{1}{\sqrt{1+(2\omega\gamma)^2}}+0.01\right] \quad (2\omega\gamma\leqslant 4). \tag{24}$$

Fitting curve A to Eq. (24) in the frequency range $0<2\omega\gamma<4$ yields κ, γ, and C_p that are all within 0.1% of their true values. In this case, the error introduced by truncating the $n<1$ terms becomes negligibly small comparison with errors of other sources, such as from the size estimation.

If one truncates the $n>1$ terms in Eq. (14) to calculate the temperature fluctuation, the error will be more significant than truncating the $n>1$ terms in Eq. (16). This is because the summation converges as n^{-3} in Eq. (14), not as n^{-4} in Eq. (16).

V. RADIAL HEAT LOSS

In the previous discussion, we have neglected the radial heat loss through radiation. Such heat loss per unit length from a cylindrical rod of diameter D to the environment of temperature T_0 can be expressed as

$$W(x,t)=\pi\epsilon\sigma D[T^4(x,t)-T_0^4]\approx 4\pi\epsilon\sigma D T_0^3\Delta(x,t), \tag{25}$$

where $\sigma=5.67\times 10^{-8}\,\text{W/m}^2\text{K}^4$ is the Stefan–Boltzmann constant, and ϵ is the emissivity.

Considering such heat loss, Eqs. (3) and (4) can be rewritten as

$$\frac{\partial}{\partial t}\Delta(x,t)-\alpha\frac{\partial^2}{\partial x^2}\Delta(x,t)+(g-c\sin^2\omega t)\Delta(x,t) = b\sin^2\omega t, \tag{26}$$

$$\begin{cases}\Delta(0,t)=0\\ \Delta(L,t)=0\\ \Delta(x,-\infty)=0,\end{cases} \tag{27}$$

where $g=16\epsilon\sigma T_0^3/\rho C_p D$. Equation (9) then becomes

$$\sum_{n=1}^{\infty}\left[\frac{dU_n}{dt}+\left(\frac{n^2}{\gamma}+g-c\sin^2\omega t\right)U_n\right]\sin\frac{n\pi x}{L}=0. \tag{28}$$

Now if we truncate the $n>1$ terms again and replace the factor $1/\gamma+g$ with $1/\gamma_{\text{ap}}$, Eq. (28) will take the similar form as Eq. (9). The final approximation solution is therefore

$$V_{3\omega}\approx\frac{4I^3LRR'}{\pi^4 S\kappa_{\text{ap}}\sqrt{1+(2\omega\gamma_{\text{ap}})^2}}, \tag{29}$$

$$\tan\phi\approx 2\omega\gamma_{\text{ap}}, \tag{30}$$

where $\kappa_{\text{ap}}=(1+g\gamma)\kappa$ is the apparent thermal conductivity, and $\gamma_{\text{ap}}=\gamma/(1+g\gamma)$ is the apparent thermal time constant of the specimen. The apparent dc temperature accumulation is $\Delta_0^{\text{ap}}=\Delta_0/(1+g\gamma)$ at the center of the specimen.

Obviously, radiation heat loss can be neglected if

$$g\gamma\ll 1. \tag{31}$$

For a cylindrical rod, condition (31) becomes $16\epsilon\sigma T_0^3L^2/\pi^2\kappa D\ll 1$, which means that the radiation power inhomogeneity caused by the temperature fluctuation along the specimen should be much less than the axial heat current or the total heating power.

Condition (31) is usually held for measurements performed below room temperature. For example, if one has a specimen of the size $L=1$ mm and $D=10^{-2}$ mm, and assuming $\kappa=100\,\text{W/m K}$, $T_0=300\,\text{K}$, the product $g\gamma$ is only around 2.5×10^{-3} even if using the emissivity of a black body.

However, for specimens of significantly longer or thinner, or if the measurement is performed at significantly higher temperatures, condition (31) will be violated. In these cases, the apparent thermal conductivity is larger than the actual value by an amount due to the radial heat loss, for cylindrical rod which is

$$\kappa_{\text{ap}}=\kappa(1+g\gamma)=\kappa+\frac{16\epsilon\sigma T_0^3L^2}{\pi^2 D}. \tag{32}$$

If one knows the emissivity, then both κ and C_p of the specimen can be calculated. Otherwise if the emissivity is unknown, one will lose the information of κ. Nevertheless, one can still get C_p of the specimen. The reason is, by substituting κ_{ap} and γ_{ap} into Eq. (20) as if there is no radial heat loss, the $(1+g\gamma)$ factors in κ_{ap} and in γ_{ap} just cancels out, which yields the correct value of C_p:

$$C_p=\pi^2\gamma_{\text{ap}}\kappa_{\text{ap}}/\rho L^2\equiv\pi^2\gamma\kappa/\rho L^2. \tag{33}$$

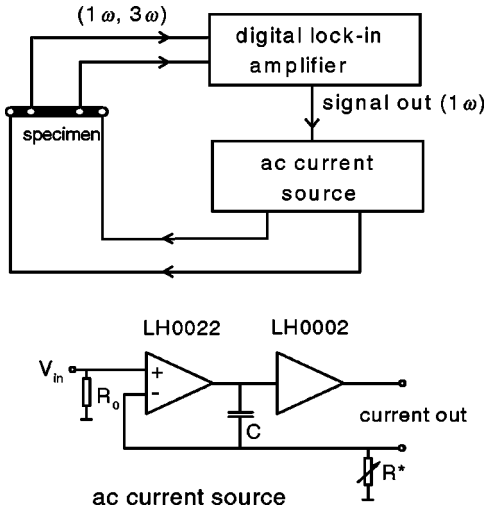

FIG. 4. Block diagram of the measurement is presented. We chose a digital lock-in amplifier SR830 or SR850 to measure the 3ω voltage. The 1ω voltage from the sine out of the lock in was boosted into an ac current by a simple electronic circuit (lower panel). It was then fed into the specimen. The feed-back resistor R* should be nearly temperature independent to prevent it from generating a 3ω component in the current.

Although this analysis is made for cylindrical rod, the conclusions are also revelatory for specimens of other shapes. One can easily deduce the factor $g\gamma$ for particular specimens if needed.

Another kind of radial heat loss, the heat loss through gas convection, also introduces a linear-term correction to the heat conduction equation. The final solution is therefore the same as Eqs. (29) and (30) except that now $g = 4\eta/\rho C_p D$ for the cylindrical specimen of diameter D (where η is the surface thermal conductivity). Similar to the case of radiation heat loss, one needs to know η before being able to calculate κ. But one can still obtain C_p of the specimen through Eq. (33) without knowing η. This has been proven to be true experimentally, even when the heat loss through gas convection is much larger than the axial thermal current (the experimental data will be shown in Fig. 7).

For eliminating the heat loss through gas convection, one simply needs a high vacuum. For eliminating radiation heat loss, however, simply using a radiation shielding at the substrate temperature T_0 would be useless because it is the radiation power inhomogeneity along the specimen that matters. Nevertheless, we feel that a simple heat shielding at T_0 will at least help minimize the static radial heat current from the specimen to the environment, especially for measurements performed above room temperature. Otherwise, such heat current could cause the temperature of the specimen to be inaccurate and the whole heat conduction processes becomes complicated.

VI. EXPERIMENTAL TESTS AND TIPS

We have tested this 3ω method on two kinds of specimens: platinum wires and bundles of multiwall carbon nanotubes, by just using the approximation solution (19). The electrical resistance of the former specimen has a positive temperature coefficient, and the latter; a negative one. Within appropriate ranges of frequency and current, we do find that $V_{3\omega} \propto I^3$ and $V_{3\omega} \propto 1/\sqrt{1+(2\omega\gamma)^2}$. For the platinum specimen, the apparent specific heat and thermal conductivity as well as the Wiedemenn–Franz ratio agree with the standard data over the entire temperature range measured (10–320 K).

Figure 4 shows the block diagram for the measurement. A digital lock-in amplifier such as a SR830 or SR850 made by Stanford Research Inc. was selected. All the filters on the lock-in were turned off, and the dc coupled input mode was selected, to ensure the observation of a true frequency dependence of $V_{3\omega}$. Before measuring the 3ω signal, the phase of the lock-in amplifier was adjusted to zero according to the 1ω voltage component. The phase angle of $V_{3\omega}$ is then $-\phi$ if $R'<0$ or $180°-\phi$ if $R'>0$ according to Eq. (17). We used a simple electronic circuit (the lower panel of Fig. 4) to convert the 1ω sine wave voltage from the sine out of the lock in to an ac current, and then we fed the current into the specimen. The 3ω component in the current was below 10^{-4} compared to its 1ω component, checked by a HP89410A spectrum analyzer. Because the 3ω voltage signal is deeply buried in the 1ω voltage signal, a certain amount of dynamic reservation is required for the lock in if, in order to keep the simplicity of this method, one is not using a bridge circuit to cancel out the 1ω signal. We kept the dynamic reservation unchanged relative to the total magnification of the lock in during the entire measurement.

There are two ways to perform the measurement. In the first, the substrate of the specimen is maintained at fixed temperatures, then the frequency dependence of $V_{3\omega}$ is measured. In this way, we can check the I^3 and the $1/\sqrt{1+(2\omega\gamma)^2}$ dependencies of $V_{3\omega}$ as well as the relation $\tan\phi = 2\omega\gamma$.

Because $V_{3\omega} \propto I^3$, one will get a much larger signal by using a larger I. However, there are three reasons for not using a very large I. First, it is required by condition (10). Second, radiation heat loss will be significant when the temperature modulation is large, as condition (31) indicates. Third, excessive heat accumulation on the specimen would even create a considerably large temperature gradient at the silver paste contacts, which might violate the boundary condition in Eq. (2). In all the cases, the expected relations such as $V_{3\omega} \propto I^3$ will not be held. On the other side, the relation will also be violated if I is too small so that $V_{3\omega}$ becomes comparable to, or even smaller than the spurious 3ω signals that come from the current or other sources. In our measurement, the total heating power was maintained such that the temperature modulation along the specimen was around 1 K. Nevertheless, if the 3ω voltage is too small to measure then one has to increase the current for creating a larger temperature fluctuation. In this case, the actual (averaged) temperature of the specimen has to be corrected afterwards by comparing the resistance of the specimen measured with the larger current and that measured with a much smaller one.

From Eq. (21), a longer and thinner specimen also gives a larger signal. However, a larger L corresponds to a larger thermal time constant γ ($\gamma \propto L^2$), and hence, a lower frequency window for measurement. In practice, it will be inconvenient to perform the measurement below 1 Hz. A larger length and a smaller cross section or diameter could also violate the conditions (10) and (31), and thus violate the

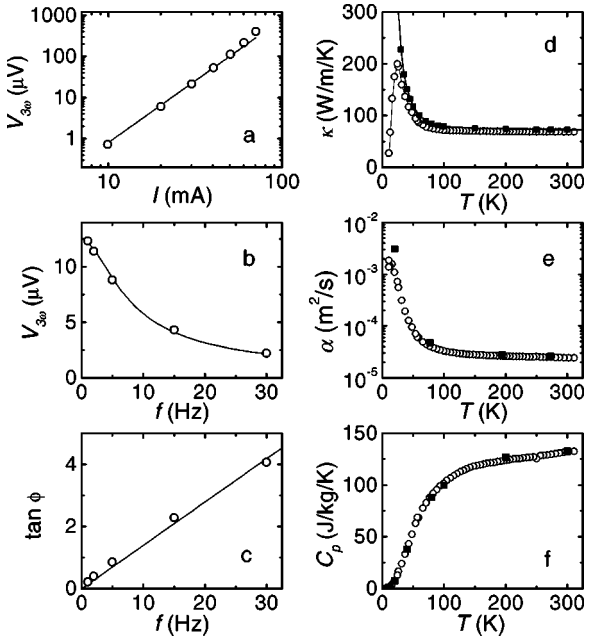

FIG. 5. Experimental test of the 3ω method on a platinum wire of 20 μm in diameter is shown. (a) The current dependence of $V_{3\omega}$. The open circles are the measured data at 25 K and 2 Hz, and the solid line is the predicted relation $V_{3\omega} \propto I^3$. (b) The frequency dependence of $V_{3\omega}$ at 25 K (open circles). The solid line is the predicted relation $V_{3\omega} \propto 1/\sqrt{1+(2\omega\gamma)^2}$. (c) The frequency dependence of the phase angle of $V_{3\omega}$ at 25 K (open circles). The obtained thermal conductivity κ, thermal diffusivity α, and specific heat C_p of the platinum specimen are plotted as open circles in (d), (e), and (f), respectively. Also shown in (d), (e), and (f) as solid squares are the standard data of platinum from literature (Ref. 12). The difference in κ and α between our data and the standard ones should reflect the difference in purity and/or structural perfection between the platinum specimens of different sources.

expected I^3 and the $1/\sqrt{1+(2\omega\gamma)^2}$ dependencies of $V_{3\omega}$.

In the second way of measurement, the temperature of the substrate is slowly ramped up or down at a fixed rate, meanwhile the working frequency of the lock-in amplifier is switched between a few set values. The maximum working frequency is adjusted by keeping $2\omega\gamma<4$ (i.e., $\phi<76°$ according to Eq. (18)). And, the electric current is adjusted roughly to maintain a fixed dc temperature accumulation (i.e., $\sim$1 K). The whole process, including the temperature ramping, parameters adjusting, and frequency switching, are all controlled by a personal computer.

For the platinum specimen, we chose a wire of diameter $D=20\ \mu$m and length $L=8$ mm. We found that the thermal time constant γ of the specimen varied from $0.005\ \mathrm{s}^{-1}$ at 10 K to $\sim 0.2\ \mathrm{s}^{-1}$ at room temperature, so that the working frequencies were chosen to be between 1 and 80 Hz. Shown in Fig. 5(a) is the current dependence of $V_{3\omega}$ at 25 K, demonstrating an I^3 dependence in a mediate current range. Figures 5(b) and 5(c) show the frequency dependencies of the amplitude and the phase angle of $V_{3\omega}$ at 25 K, compared with the predicted functional forms (the solid lines). By fitting the data in Fig. 5(b) to Eq. (19), we obtained the thermal conductivity κ [Fig. 5(d), open circles] and the thermal time constant γ. The thermal diffusivity and the specific heat of the specimen can be obtained by using the relations $\gamma = L^2/\pi^2\alpha$ and $\alpha=\kappa/\rho C_p$. The results are shown in Figs. 5(e) and 5(f) as open circles. C_p thus obtained agrees well with the standard data for platinum[12] [the solid squares in Fig. 5(f)].

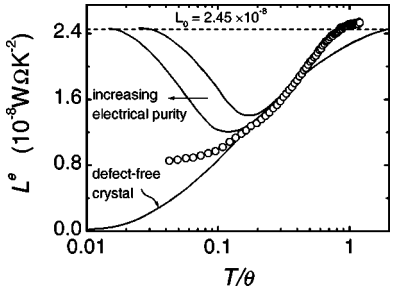

FIG. 6. The Wiedemenn–Franz ratio L^e of our platinum specimen compared with that of usual metals with different purity is shown. The result indicates that the platinum wire used in this experiment is pure but not totally defect free. The room temperature Wiedemenn–Franz ratio of the platinum wire is about $2.52\times10^{-8}\ \mathrm{W\Omega/K^2}$, which is in good agreement with the reported value of $2.6\times10^{-8}\ \mathrm{W\Omega/K^2}$ in literature (Ref. 14). The Lorenz number of free electron gas is $L_0=2.45\times10^{-8}\ \mathrm{W\Omega/K^2}$, plotted as the dashed line. Note that for platinum, the Debye temperature θ is 240 K.

The thermal conductivity of our platinum wire shows a less pronounced peak at low temperatures compared to that of high purity platinum. Since κ depends largely on the purity, structural perfection, and even the size of the specimen, we think that the κ data we obtained reflect the true thermal conductivity of our platinum wire. In fact, the Wiedemenn–Franz ratio of the specimen deduced from the thermal conductivity and the electrical resistivity, or more directly, deduced from the thermal conductance and the electrical resistance, fits the case of pure but not totally defect-free metals,[13] as shown in Fig. 6. The Wiedemenn–Franz ratio is found to be $\sim 2.53\times10^{-8}\mathrm{W\Omega/K^2}$ at 290 K. It is slightly larger than the free-electron Lorenz number $2.45\times10^{-8}\ \mathrm{W\Omega/K^2}$, and is rather close to $2.6\times10^{-8}\ \mathrm{W\Omega/K^2}$, the reported value in literature for platinum.[14]

Let us now examine the effect of radial heat loss through gas convection. The data in Fig. 5 were taken in a high vacuum where such heat loss was virtually absent, as that changing the vacuum pressure by a factor of 2 yielded a same κ. Shown in Figs. 7(a)–7(c) are two sets of data taken on another platinum specimen at two different vacuum pressures. The circles represent the data taken in a vacuum where radial heat loss emerged but was not severe (indicated by the slightly positive slope of κ at at high temperatures). During one of the warming-up measurements, however, we introduced radial heat loss by destroying the vacuum of the system. After that, spurious larger thermal conductivity and diffusivity of the specimen were obtained, shown as the squares in Figs. 7(a) and 7(b). The radial heat current reached several times larger than the axial one at room temperature, as indicated in Fig. 7(a). Nevertheless, the specific heat deduced from κ and α was quite insensitive to the radial heat loss [Figs. 7(c)]. The reason has been explained in Sec. V.

After all, let us check if conditions (10) and (31) were satisfied. If taking $n=1$, we had $I_0^2 R' L/n^2\pi^2\kappa S \sim 10^{-5}$. Therefore, condition (10) was well satisfied. For condition (31), assuming an emissivity $\epsilon=1$ for our platinum wire leads to $g\approx 0.44\ \mathrm{s}^{-1}$ at 300 K. On the other hand, γ (actually,

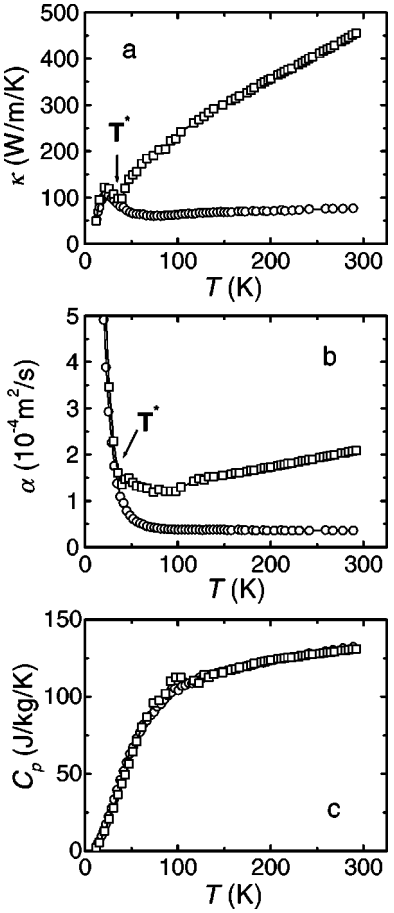

FIG. 7. The effect of radial heat loss through air convection is presented. The circles represent the data taken in a vacuum where radial heat loss was not significant. In one warming-up run of the measurement, radial heat loss was triggered on above T^* by destroying the vacuum of the system. The heat loss resulted in a spurious larger thermal conductivity and diffusivity for the specimen [the squares in (a) and (b)]. But, as predicted by Eq. (33), the specific heat deduced from them was relatively insensitive to such heat loss [the squares in (c)].

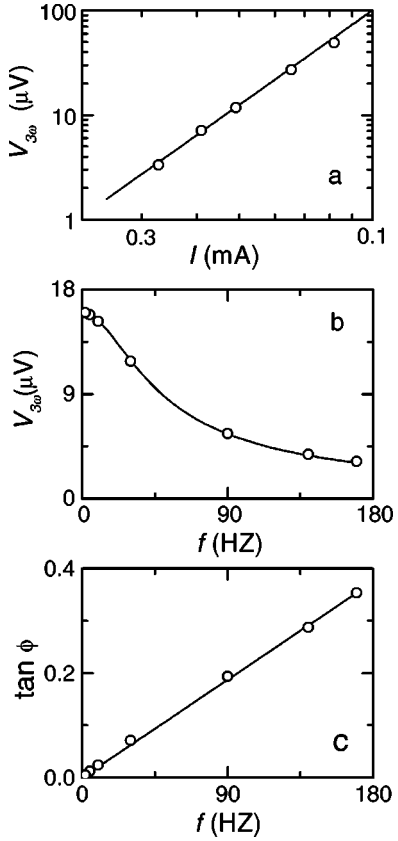

FIG. 8. Experimental test of the 3ω method on multiwall carbon nanotube bundles at 50 K is shown. (a) The current dependence of the 3ω voltage measured at 10 Hz compared with the predicted form $V_{3\omega} \propto I^3$ (the solid line). (b) The frequency dependence of $V_{3\omega}$ compared with the predicted relation $V_{3\omega} \propto 1/\sqrt{1+(2\omega\gamma)^2}$. (c) The frequency dependence of the phase angle of $V_{3\omega}$ compared with the predicted relation $\tan\phi \propto \omega$. The temperature dependencies of the thermal conductivity, thermal diffusivity and specific heat of the material have already been published elsewhere (Ref. 15).

γ_{ap}) deduced from the measurement was ~ 0.2 s. Therefore, $g\gamma \approx 0.088$. In the real case, the product $g\gamma$ should be much smaller than 0.088, because the emissivity of a shiny metal is usually much less than unity. Therefore, condition (31) should also be well satisfied.

We have also applied the 3ω method to measure the κ and C_p of multiwall carbon nanotube (MWNT) bundles who have a negative R' (Ref. 15). MWNT is a highly anisotropic material both in geometry and in thermal conductivity, owing to its strong in-plane sp^2 bonding and the weak interwall van der Waals bonding. Its macroscopic length against the nanometer-sized diameter overall ensures a much shorter thermal time constant in the radial direction than in the axial direction. We believe this conclusion is also true for a bundle of MWNTs. Therefore the heat conduction can be regarded as a 1D problem. For MWNTs there are no C_p and κ data from other sources available for comparison. Nevertheless, the obtained frequency and current dependencies of $V_{3\omega}$ were all in good agreement with Eq. (19) (Fig. 8), which guarantees the reliability of κ and C_p thus obtained. For a carbon nanotube bundle of $L=1$ mm and $D=10\,\mu$m, $I_0^2 R' L/\pi^2 \kappa S$ was less than 10^{-3} at temperatures above 60 K, and was about 0.08 at 10 K. In addition, the product $g\gamma$ was below 4×10^{-3} in the whole temperature range investigated (estimated using the emissivity of a black body). Therefore, both conditions (10) and (31) were satisfied if considering the bundle as a unitary object. The nanotubes inside the bundle were actually ''self-shielded'' by the outmost ones if examining them individually, which might effectively eliminate the radial heat loss.

For a carbon nanotube bundle of 1 μm in diameter and 1 mm in length, its mass is only around 10^{-9}g, far less than the minimum amount of mass (typically in mg) required in many other kinds of C_p measurement.

VII. DISCUSSION

We have explored a 3ω method for measuring the thermal conductivity and specific heat of a rod or filament-like specimen. By fitting the frequency-dependent 3ω voltage data to Eq. (19) within the frequency range $0<2\omega\gamma<4$, we can obtain κ and C_p of the specimen to an accuracy of 2%–4%. For achieving a higher accuracy, one can fit the data to Eq. (24). The presence of radial heat loss will result in a larger apparent thermal conductivity. But C_p obtained by this method is very much insensitive to such heat loss and thus maintains reliability. A successful measurement relies on

properly choosing the dimensions of the specimen so that one can have a large enough 3ω voltage, yet maintain a convenient working frequency range and keep condition (10) [and condition (31), if necessary] satisfied.

ACKNOWLEDGMENTS

The authors thank G. H. Li and X. N. Jing for helpful discussions. This work was supported by NSFC, and by the President's Foundation of CAS.

[1] O. M. Corbino, Phys. Z. **11**, 413 (1910).
[2] L. R. Holland, J. Appl. Phys. **34**, 2350 (1963).
[3] D. Gerlich, B. Abeles, and R. E. Miller, J. Appl. Phys. **36**, 76 (1965).
[4] L. R. Holland and R. C. Smith, J. Appl. Phys. **37**, 4528 (1966).
[5] D. G. Cahill and R. O. Pohl, Phys. Rev. B **35**, 4067 (1987).
[6] N. O. Birge and S. R. Nagel, Rev. Sci. Instrum. **58**, 1464 (1987).
[7] D. G. Cahill, E. Fischer, T. Klitsner, E. T. Swartz, and R. O. Pohl, J. Vac. Sci. Technol. A **7**, 1259 (1989).
[8] D. G. Cahill, Rev. Sci. Instrum. **61**, 802 (1990).
[9] R. Frank, V. Drach, and J. Fricke, Rev. Sci. Instrum. **64**, 760 (1993).
[10] D. H. Jung, T. W. Kwon, D. J. Bae, I. K. Moon, and Y. H. Jeong, Meas. Sci. Technol. **3**, 475 (1992).
[11] As we will see in Figs. 5(b) and 8(b) in Sec. VI, there is always some small but systematic deviation at high frequencies if fitting our experimental data to Eq. (19). Such a deviation can be reduced by fitting the data to Eq. (24).
[12] R. J. Corruccini and J. J. Gniewek, *CRC Handbook of Chemistry and Physics* (CRC Press, Boca Raton, FL, 1988), p. D-181.
[13] R. Berman, *Thermal Conduction in Solids* (Oxford University Press, New York, 1978), p. 152.
[14] J. P. Moore, D. L. McElroy, and M. Barisoni, Proceedings of the Sixth Thermal Conductivity Conference, Dayton, Ohio, p. 737.
[15] W. Yi, L. Lu, Z. Dian-Lin, Z. W. Pan, and S. S. Xie, Phys. Rev. B **59**, R9015 (1999).